AIAA 80-0115R

Navigation Accuracy Analysis for an Ion Drive Flyby of Comet Halley

Lincoln J. Wood*
Jet Propulsion Laboratory, California Institute of Technology, Pasadena, Calif.

A dual comet (Halley flyby/Tempel 2 rendezvous) mission, making use of the solar electric propulsion system, was recently considered for a 1985 launch. This paper presents navigation accuracy analysis results for the Halley flyby phase of this mission. Orbit determination and guidance accuracies are presented for the baseline navigation strategy, along with the results of a number of sensitivity studies involving parameters such as data frequencies, data accuracies, ion drive thrust vector errors, comet ephemeris uncertainties, time lags associated with data processing and command sequence generation, probe release time, and navigation coast arc duration.

Introduction

COMETARY exploration by means of unmanned spacecraft has been strongly endorsed by the space science community for a number of years. Various missions have been considered by NASA, including a 1980 Comet Encke rendezvous,[1,2] a 1980 Comet Encke slow flyby,[1,3] and a 1985 Comet Halley rendezvous.[4,5] Recently under consideration has been a mission to two comets, Halley and Tempel 2.[6,7] This mission would have included a fast flyby of the comet Halley, coupled with delivery of an atmospheric probe to the vicinity of the cometary nucleus, followed by a rendezvous with the comet Tempel 2 several years later.

Among the scientific objectives of cometary missions are the determination of the chemical composition and physical structure of cometary nuclei and atmospheres, investigation of the dynamic processes occurring at the surfaces of nuclei and within the atmospheres, and investigation of the interaction of comets with the solar wind, including study of the formation and structure of cometary tails.[8] This dual comet mission is particularly attractive scientifically because the comets Halley and Tempel 2 are quite different in nature, Halley being very active near perihelion, Tempel 2 being relatively inactive.

This mission would have been made possible with the use of the solar electric propulsion system (SEPS). Comet rendezvous missions are very difficult to perform in a ballistic manner, due to the excessive amount of chemical propellant required.[6] During calendar year 1980, emphasis in comet mission planning has shifted away from this dual comet mission to two separate missions, a ballistic flyby of Comet Halley,[9,10] followed several years later by an electric propulsion rendezvous with a short-period comet, such as Comet Tuttle-Giacobini-Kresak.[11] This change in emphasis was motivated by uncertainties in SEPS funding for fiscal year 1981 and thereafter, which might have precluded SEPS availability for the dual comet mission. The dual comet mission is still of considerable interest, however, since it was analyzed in some detail and is representative, in many respects, of SEP cometary missions in general.

The mission plan in the Halley flyby/Tempel 2 rendezvous mission calls for a single flight system to be launched by the Space Shuttle/Inertial Upper Stage in the summer of 1985. The flight system consists of a SEPS, a rendezvous spacecraft, and a Halley atmospheric probe. The fast flyby (58 km/s) of Halley occurs only 4 months after launch, prior to Halley perihelion. The nonmaneuvering Halley probe is released from the spacecraft 15 days before Halley encounter to acquire data on a ballistic path through the atmosphere of Halley. After probe release, the rendezvous spacecraft is deflected by the SEPS for safe flyby to the sunward side of Halley, outside the dust envelope. The spacecraft makes remote observations of Halley during the flyby and serves as a relay link for data acquired by the probe. Rendezvous with Tempel 2 requires a total flight time of nearly 3 years.

Up to the time of rendezvous, the SEPS provides a virtually continuous low level of thrust. Nonthrusting periods are limited to brief intervals required for accurate orbit determination prior to Halley probe release, for Halley encounter data acquisition, and for occasional engineering and science instrument calibrations. The number of operating thrusters, thruster throttle levels, and thrust directions are optimized, subject to certain constraints, in order to maximize the rendezvous spacecraft payload, with time of rendezvous assumed fixed.

An ecliptic plane projection of the heliocentric trajectory is shown in Fig. 1. The mission can be divided into six phases: launch, initial SEP cruise, Halley flyby, second SEP cruise, Tempel 2 rendezvous approach, and Tempel 2 operations. In Ref. 12, an overall navigation system design was presented. Navigation strategies for each of these mission phases were discussed, and some preliminary navigation accuracy assessments presented. In Ref. 11, the Tempel 2 rendezvous approach phase was examined in detail (along with the corresponding phase of a mission to Comet Tuttle-Giacobini-Kresak). Orbit determination and guidance accuracies were obtained for the baseline navigation strategy, and a number of sensitivity studies involving parameters such as data frequencies, data accuracies, ion drive thrust vector errors, comet ephemeris uncertainties, time lags associated with data processing and command sequence generation, and limits placed on thrust vector changes for guidance purposes were carried out.

In this paper, the Halley flyby phase is examined in detail. Orbit determination and guidance accuracies are obtained for the baseline navigation strategy. Sensitivity studies involving parameters, such as those mentioned above for the Tempel 2 rendezvous approach phase, as well as time of probe release and navigation coast arc duration, are described.

Navigation System Design

The navigation system for this mission consists of the Deep Space Network (DSN), elements of the flight system (spacecraft and SEPS), ground-based astronomical observatories, and ground-based computational facilities and software. The DSN will provide various radiometric data

Presented as Paper 80-0115 at the AIAA 18th Aerospace Sciences Meeting, Pasadena, Calif., Jan. 14-16, 1980; submitted Feb. 26, 1980; revision received Oct. 15, 1980.

*Member Technical Staff, Navigation Systems Section. Member AIAA.

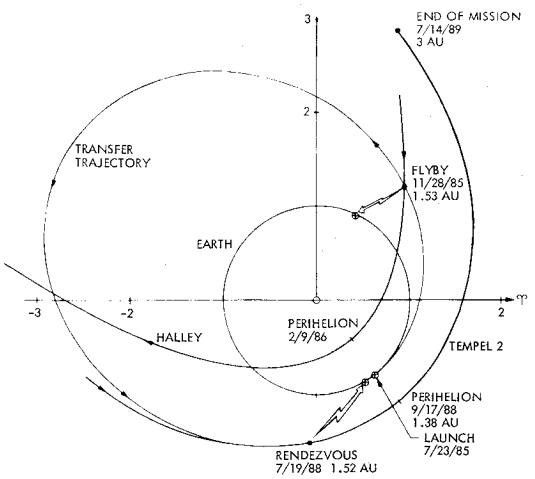

Fig. 1 Heliocentric trajectory (ecliptic plane projection).

types for orbit determination purposes. These data types include two-way doppler and range, multistation differenced doppler (two-way minus three-way), and multistation differenced range. It is planned that these radiometric data types will be packaged in the form of navigation tracking cycles. A navigation tracking cycle consists of four consecutive overlapping passes of dual frequency (S-band uplink and S/X-band downlink) coherent range and doppler data with simultaneous doppler and near-simultaneous range acquired during the overlapping station view periods. The tracking cycle is enhanced if it begins and ends with southern hemispheric coverage (Australia) to balance the northern hemispheric coverage. The dual frequencies are used to calibrate the radio data for the effects of charged particles in the transmission media (interplanetary space plasma, Earth's ionosphere, ion thruster exhaust plasma, and near-comet environment). The simultaneous doppler data constitute a useful radiometric data type because of their insensitivity to unmodeled accelerations. The simultaneous range data are useful for estimating spacecraft geocentric declination when it is close to zero. Although not presently included in the baseline navigation system design, narrow- or wide-band differential very-long-baseline interferometry (ΔVLBI) could also be used as a radiometric data type.

The portions of the flight system which may be considered part of the navigation system include various sensors which produce data useful for orbit determination (the imaging subsystem and, if included onboard, a radar ranging subsystem, and an accelerometer), and the thrust subsystem of the SEPS, which provides the means of effecting trajectory changes. Each of these subsystems or instruments, while important for navigation, serves other functions as well.

Optical navigation data consist of images of the cometary nucleus against a background of catalogued stars. Such images are recorded using the appropriate focal length optics in the spacecraft imaging subsystem, in conjunction with a charge-coupled device photodetector (1000×1000 array). An image of this sort, after suitable processing, yields a fairly accurate estimate of the flight system's position relative to the nucleus in the directions perpendicular to the line of sight. Little useable flight system/comet range information is contained in a single image. The processing of a set of images taken as the flight system/comet relative geometry changes enables range to be inferred, however. The onboard optical data will be complemented by ground-based comet observations (photographic plates recorded at astronomical observatories).

When the flight system is sufficiently near a cometary nucleus, the onboard optical data may be augmented by flight system/nucleus range data provided by an X-band radar altimeter. An altimeter will not be of any use during the Halley flyby mission phase, however, due to the large separation between the flight system and the cometary nucleus even at closest approach (130,000 km).

It is desired that nongravitational accelerations of the flight system (due to thrust and solar radiation pressure) be determinable from SEPS telemetry data to an accuracy of 10^{-6} m/s^2, in each of three inertially fixed directions, during the thrusting portions of the Halley flyby phase, and to an accuracy of 10^{-7} m/s^2 during the nonthrusting portions. It is also desired that the thrust acceleration of the flight system be controlled to an accuracy of 3×10^{-6} m/s^2, in each of three inertially fixed directions, during this mission phase. It is furthermore desired that the brief trim maneuver prior to Halley probe release be executed to an accuracy of 2%. These specifications, and analogous specifications for other mission phases, may require the inclusion of a three-axis accelerometer onboard the SEPS. Telemetry data from the SEPS attitude and articulation control and thrust subsystems will also be needed on a timely basis for navigation purposes.

During powered flight mission phases (all phases except the Tempel 2 operations phase), estimated trajectory dispersions (i.e., errors in the position and velocity of the flight system) are corrected by suitably modifying the thrust vector history up to the time of initial rendezvous (and perhaps shifting the time of rendezvous also). During the Tempel 2 operations phase (and shortly before Halley probe release), trajectory corrections will be made by means of discrete thrusting maneuvers, as in a ballistic mission, except that the thrust levels will be small, due to the use of the ion thrusters. It is currently envisioned that the SEPS will have eight thrusters, a maximum of seven of which will be used at any one time during a cometary mission. The ground-based operational orbit determination and guidance functions and associated computational software for an electric propulsion comet rendezvous mission are described briefly in Ref. 12.

Two mission options, the so-called "maximum" and "minimum" missions, differing according to sophistication of science objectives and flight system design, have been considered for the dual comet mission. The "maximum" spacecraft design includes a radar altimeter, a dual frequency (S/X-band) downlink capability, and three imaging systems (focal lengths of 3000, 600, and 140 mm). The "minimum" spacecraft design does not include a radar altimeter, includes only a single frequency (S-band) downlink capability, and includes two imaging systems (focal lengths of 3000 and 300 mm). (Only those differences which are pertinent to navigation are listed here.)

Navigation Strategy

The Halley flyby mission phase begins 50 days before Halley encounter, at which time Halley should be detectable with the 3000-mm focal length solid-state imaging system onboard the spacecraft. At this time, the radio tracking activity will be stepped up. Navigation tracking cycles will be scheduled every 5 days. A single station pass of two-way coherent doppler data, with ranging, will be needed each day, outside of the navigation tracking cycles. Ground-based observations of Halley will begin somewhere between 50 and 100 days prior to Halley encounter and will be repeated at 5-day intervals until the end of the mission phase. These observations will help to reduce the large ephemeris uncertainty of Halley.

For the first 10 days of this mission phase, optical navigation imaging frames will be recorded twice a day. After the first several navigation imaging frames have been acquired and an orbit determination solution obtained, the trajectory will be retargeted (i.e., a new nominal trajectory and a corresponding thrust vector history will be searched out). Subsequent to this trajectory retargeting, the thrust vector commands will be periodically updated (every 5 days, after a navigation tracking cycle and a subsequent orbit determination solution) using a linear guidance scheme. The

control gains for the linear guidance will be computed only once, at the same time as the retargeting, and then stored, thus significantly reducing the computational effort during the high-activity approach period and shortening the time needed for the overall control update operation.

Beginning at 40 days prior to encounter, the number of optical navigation imaging frames taken each day will be increased from two to four. Approach phase navigation relies heavily on onboard optical observations of the cometary nucleus relative to background catalogued stars. These observations directly link the spacecraft and the target body and are extremely important because of the large cometary ephemeris uncertainty. The cometary nucleus will resemble a star in all optical navigation frames taken prior to probe release, since the angular diameter of the nucleus will be at least two orders of magnitude smaller than that of a picture element in the photodetector array.

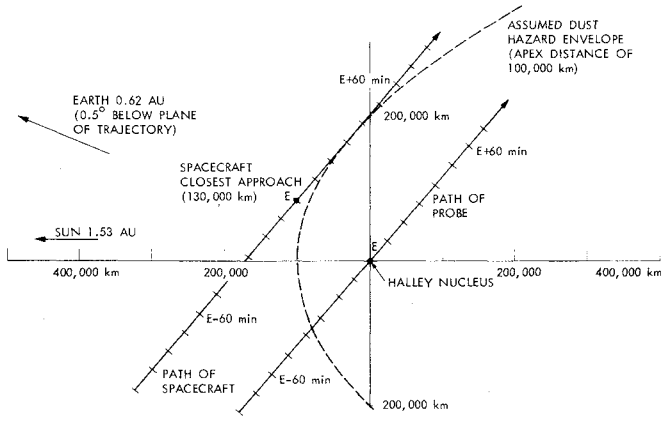

Fig. 2 Trajectories near Halley encounter.

Table 1 Orbit determination a priori error standard deviations and random process statistics

Parameter	A priori standard deviation	Correlation time
Estimated parameters		
Spacecraft position	1,000,000 km	NA
Spacecraft velocity	1 km/s	NA
Spacecraft mass	20 kg	NA
Cometary position	5000 km	NA
Cometary velocity	2.0×10^{-4} km/s	NA
Thrust acceleration fluctuations (continuous mode)	1.0×10^{-9} km/s^2 [a]	1 day
Thrust acceleration drift (continuous mode)	1.0×10^{-9} km/s^2 [a]	20 days
Thrust acceleration fluctuations (trim maneuver)	1.5×10^{-9} km/s^2 [a]	1 day
Thrust acceleration drift (trim maneuver)	1.5×10^{-9} km/s^2 [a]	20 days
Nongravitational acceleration errors during nonthrusting periods (radially away from sun)	1.0×10^{-10} km/s^2 [a]	4 days
Nongravitational acceleration errors during nonthrusting periods (nonradial components)	2.0×10^{-11} km/s^2 [a]	4 days
Considered parameters		
Station longitudes	3 m	NA
Station spin radii	1.5 m	NA
Differenced range biases	6 m [b]	NA
Differenced frequency biases	4×10^{-13} [b]	NA
Onboard camera optical biases	0.5 pixels (2.5 μrad)	NA
Probe separation velocity	10^{-5} km/s	NA

[a] Also steady-state standard deviation of random process.
[b] Correlation coefficient = −0.5.

The Halley encounter targeting objectives are to deliver a spin-stabilized, nonthrusting atmospheric probe to the vicinity of the cometary nucleus with the minimum possible miss distance, while deflecting the remainder of the flight system to a minimum safe flyby distance for remote observation of the comet and for probe data relay support. The flight system is initially targeted directly for the nucleus. Probe spinup and release are scheduled to occur about 15 days before Halley encounter.

The accuracy of the orbit determination process is dependent upon the accuracy with which nongravitational accelerations acting on the flight system are known. This is the basis for the requirement on knowledge of nongravitational accelerations which was stated in the previous section. Since these accelerations can be determined to a higher level of accuracy when the thrusters are shut off than when they are operating, a 4-day coast period is scheduled prior to probe release. Following this coast period is a brief period of thrusting (several hours in length), to correct any trajectory errors detected in the most recent orbit determination solution. This orbit determination solution will include no data taken within 24 h of the start of the maneuver, 24 h being the assumed turnaround time for processing orbit determination data, estimating flight system state and other parameters, calculating thrust vector updates, generating a maneuver command sequence, plus round-trip light time. Since the probe delivery accuracy is dependent upon the accuracy with which this final trim maneuver is executed, a requirement (stated in the previous section) has been placed on the execution accuracy of this maneuver.

Since the probe cannot be commanded after release, the reference time for the start of probe science and engineering sequences will also be updated prior to release. The attitude of the flight system will be adjusted after the trim maneuver in order to achieve the desired probe spin axis orientation. After probe release, a period of about 24 h will elapse before thrusting of the SEPS will resume. This will allow time for the probe to move far enough from the SEPS not to be damaged by subsequent thrusting (the separation velocity is less than 1

Table 2 Orbit determination data frequencies and data noise standard deviations

Data type	Data frequency	Data noise standard deviation
Range	Approximately one point every 4 h during tracking cycles	1000 m [a]
Range rate	One point per minute during tracking cycles	100 mm/s [a]
Range	Approximately one point every 4 h during daily station passes outside tracking cycles	100 m
Range rate	One point per minute during daily station passes outside tracking cycles	1 mm/s
Differenced multistation range	When available during tracking cycles	2 m
Differenced multistation range rate	When available during tracking cycles	1 mm/s
Onboard optical	Every 12 h E − 50 to E − 40 Every 6 h E − 40 to E − 15	1 pixel (5μrad)
Earth-based comet	Every 5 days after E − 55	3 arc-sec

[a] Value chosen to give correct relative weighting between conventional and differenced data types.

Table 3 Position uncertainty standard deviations and position standard deviations mapped to encounter with Halley

Time	Mapped position uncertainty, km			Mapped position, km		
	Downtrack	Crosstrack	Out-of-plane	Downtrack	Crosstrack	Out-of-plane
E − 45.75	7514	3139	4744	7514	3139	4744
E − 40.75	6016	2104	3028	7657	3768	4948
E − 35.75	5391	1634	2229	7972	3349	4041
E − 30.75	4795	1233	1632	8334	2931	3355
E − 25.75	4153	894	1175	8677	2512	2800
E − 20.75	3450	622	846	8966	1808	2032
E − 19.50	3471	611	864	9028	710	951
E − 15.50	2670	316	360	9028	711	951
E − 15.25	2660	294	328	9028	322	365
E − 15.00	2029	281	319	9028	322	365
E	1128	266	271	9028	322	365

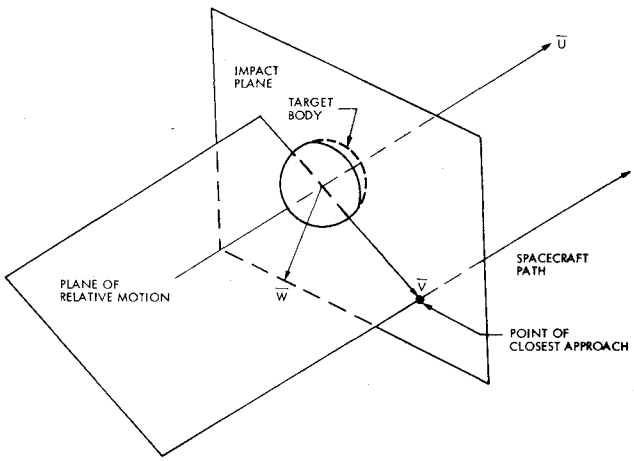

Fig. 3 Impact plane coordinate system.

m/s). In order for the flight system to clear the Halley dust envelope, which has an estimated apex distance of 100,000 km relative to the nucleus, it is necessary to thrust for about 9 days. The thrusters will be turned off for 10 days centered about Halley encounter, to allow science sequences to be performed. Trajectories of the probe and the spacecraft/SEPS near Halley encounter are shown in Fig. 2.

After probe release, the number of optical navigation imaging frames taken each day will be reduced from four to two, until 10 days after closest approach, at which time optical navigation imaging will terminate. The resulting data will help to determine the position of the spacecraft relative to the comet, near encounter, and will also improve knowledge of the cometary ephemeris, since the spacecraft can be accurately tracked relative to the Earth. The knowledge of the probe trajectory relative to the comet can also be improved by suitably processing data involving the spacecraft and the comet (but not the probe) after the time of probe release.

Navigation Accuracy Analysis for Halley Probe Delivery-Baseline Case

Covariance analyses have been carried out to investigate the statistical properties of the orbit determination and guidance strategies described above for Halley probe delivery. The required computer runs were made with orbit determination and guidance software, which is simpler than, but mathematically similar to, that which may be used in mission operations.

The parameters which were estimated in carrying out the orbit determination solution were the flight system position, velocity, and mass, the cometary ephemeris, thrust acceleration errors, and, during coast arcs, other nongravitational accelerations. The solution was obtained by using a sequential filtering procedure which allows for stochastic accelerations by modeling them as first-order Gauss-Markov processes. The thrust acceleration errors were represented as independent variations in three orthogonal directions. The error in each direction was modeled as the sum of two independent Gauss-Markov processes, characterized by different correlation times, in order to represent both short- and long-term effects. Standard deviations and correlation times were taken to be the same in each direction. The nongravitational accelerations during coast arcs were modeled similarly, except that a single Gauss-Markov process was used for each acceleration component, and the three components were not treated identically.

A priori error standard deviations for the estimated parameters and correlation times for the Gauss-Markov processes are given in Table 1. The a priori error standard deviations for estimates of spacecraft position and velocity were chosen to be very large, so as to have little impact on the orbit determination results. Actual orbit determination accuracies at the end of the initial SEP cruise phase can be expected to be much better than these numbers.

Parameters which were considered, rather than estimated, in carrying out the orbit determination solution include equivalent station location errors (crust-fixed station location errors plus residual calibration errors associated with transmission media effects, polar motion, and Earth spin rate) for stations 14, 43, and 63 (errors in station spin radius and longitude were included; errors in distance above the equatorial plane were not), differenced range biases between stations 14 and 63 and between stations 43 and 63, and differenced frequency biases between the same pairs of stations. (These three stations are in the 64-m DSN subnet. The 34-m stations which would actually be used are quite nearby, however.) Also included as considered parameters were biases in the onboard optical data and errors in the probe separation velocity components.

The standard deviations associated with the noise in the various data types are presented in Table 2. The noise levels for the conventional range and range rate during tracking cycles were not set to reflect actual data accuracies, but rather to give the correct relative weightings between the conventional and differenced data types.

A batch size of 12 h was used in carrying out the orbit determination solution. Corrections in the three thrust acceleration components were computed every 5 days based upon estimated perturbations in position, velocity, and bias parameters, between E − 45.75 and E − 19.50 (E = Halley encounter; numbers represent days before encounter). These control corrections were chosen to be piecewise constant over 2½-day intervals. Standard deviations of control corrections were limited to 2×10^{-8} km/s^2 (roughly 10% of the nominal thrust acceleration) in each direction.

Between E − 19.50 and E − 15.50, no control corrections were allowed, since the ion engines are to be turned off during this time to allow improved orbit determination accuracy. Between E − 15.50 and E − 15.25, a single constant control correction was allowed (this represents the final trim maneuver). No control corrections were allowed after E −

15.25. Probe separation was assumed to occur at E − 15. No disturbances to the probe trajectory were modeled after separation. A variable time-of-arrival mode of the minimum miss terminal guidance technique described in Refs. 13 and 14 was the perturbation guidance technique employed.

In Table 3, standard deviations of the spacecraft position uncertainty and the spacecraft position, both mapped deterministically from the current time to the time of encounter, are presented. Note that the spacecraft state is referenced to that of the comet, not to that of the sun or Earth. The spacecraft state uncertainties (or orbit determination errors) are those errors associated with the spacecraft state estimate at time t, based on data through time t minus 1 day, one day being the assumed data turnaround time for guidance purposes. The spacecraft state errors represent trajectory dispersions, i.e., deviations of the actual trajectory from the nominal trajectory. Downtrack, crosstrack, and out-of-plane directions correspond to the unit vectors $\bar{U}$, $\bar{V}$, and $\bar{W}$ shown in Fig 3.

It can be seen in Table 3 that the mapped crosstrack and out-of-plane position uncertainty standard deviations continually decrease from E − 45.75 to E − 19.50. The mapped downtrack position uncertainty standard deviation does not decrease as rapidly as the crosstrack and out-of-plane components, since the onboard optical data provide relatively little information in the downtrack direction. What improvement there is comes largely from ground-based comet observations. The mapped crosstrack and out-of-plane position standard deviations also decrease, generally, during this time interval, as control corrections are applied, based upon improving estimates of the state and bias parameters. The mapped downtrack position standard deviation does not decrease, however, due to the fact that no effort is made to control this position error component. The probe miss distance at the time of closest approach is of extreme importance, but the time of closest approach itself is not (unless the timing is far enough off to adversely affect probe science sequences). For this reason, the time of encounter is allowed to vary freely, and all control effort is directed toward minimizing the probe miss distance. The corrections required were less than the limits imposed throughout this period of time.

The mapped crosstrack and out-of-plane position uncertainty standard deviations drop dramatically between E − 19.5 and E − 15.5. This is due to the fact that the ion engines are turned off during this time interval, so that the level of process noise is substantially reduced, enabling an improved orbit determination solution. (The importance of a navigation coast in flyby missions was first examined in detail in Ref. 3.) All mapped position standard deviations hold virtually constant during this time interval, since no control corrections are being applied. Between E − 15.5 and E − 15.25, the mapped crosstrack and out-of-plane position standard deviations decrease substantially due to the final 6-h trim maneuver, which is executed based upon the improved orbit determination solution obtained as a result of the navigation coast. Standard deviations of thrust acceleration components required for this trim maneuver were found to be 1.54×10^{-8} km/s^2, 3.15×10^{-8} km/s^2, and 1.46×10^{-8} km/s^2 in three orthogonal directions (the first component is along the flight system/sun line; the other two directions are determined by the reference star Canopus), well within the thrusting capabilities at this solar range.

Since no corrective maneuvers are applied after E − 15.25, the mapped position standard deviations are essentially constant subsequent to this time. (They cannot possibly decrease in the absence of control corrections; and in this particular circumstance, increases due to probe separation velocity errors and stochastic accelerations turn out to be negligibly small.)

Perhaps the most important entries in Table 3 are the crosstrack and out-of-plane position standard deviations at time E. These statistics imply that the probe will pass within 322 km of the Halley nucleus in the crosstrack direction with probability 68.3%, and that it will pass within 365 km of the nucleus in the out-of-plane direction with probability 68.3%. The Halley probe miss statistics can thus be described by error ellipses in the impact plane, centered at the Halley nucleus (see Fig. 3). The projections of the 1σ error ellipse onto the two axes are 322 and 365 km, respectively. The semimajor and semiminor axes of this error ellipse are 380 and 304 km, respectively. The probability that the probe will pass inside of this 1σ error ellipse is 39.4%. The probability that the probe will pass inside of an error ellipse twice as large in each dimension is 86.5%. The probability that the probe will pass inside of an error ellipse three times as large is 98.9%. Of most interest, perhaps, are not the probe miss statistics in the crosstrack and out-of-plane directions (jointly Gaussian and correlated) or the probe miss statistics in the semimajor and semiminor axis directions (jointly Gaussian and uncorrelated), but rather the radial probe miss statistics. The probability density function for radial miss distance is the product of a Rayleigh density function and a modified Bessel function. The mean radial miss distance can be determined from the expression

$$\langle r\rangle = \left(\frac{2}{\pi}\right)^{1/2}\sigma_1 E\left[\frac{(\sigma_1^2-\sigma_2^2)^{1/2}}{\sigma_1}\right]$$

where σ_1 and σ_2 are the semimajor and semiminor axes of the 1σ error ellipse, r the radial miss distance, $\langle\cdot\rangle$ the expected value, and $E[\cdot]$ the complete elliptic integral of the second kind.[15] For the case at hand, we obtain $\langle r\rangle = 394$ km. Also, the rms radial miss distance can be determined from the expression

$$\langle r^2\rangle^{1/2} = (\sigma_1^2+\sigma_2^2)^{1/2}$$

For the case at hand, $\langle r^2\rangle^{1/2} = 487$ km.

Note that the mapped position standard deviations in the crosstrack and out-of-plane directions at time E − 15.25 are only slightly larger than the corresponding mapped position uncertainty standard deviations at time E − 15.5. The differences are due to errors in the execution of the trim maneuver.

The downtrack mapped position uncertainty standard deviation at E − 15 is also an important quantity, since E − 15 is the last opportunity at which the timing of probe science sequences can be updated. Since the probe/comet relative velocity at flyby is 57.8 km/s, the 2029 km (1σ) downtrack position uncertainty is equivalent to a time-of-encounter uncertainty of 35.1 s (1σ). The downtrack mapped position standard deviation at E − 15 of 9028 km yields, similarly, the accuracy with which the time of encounter is being controlled, namely, 156 s (1σ).

It will be of considerable scientific interest to determine the position of the probe relative to the comet as accurately as possible near encounter. As can be seen from Table 3, the probe position at encounter with Halley can be predicted to an accuracy of 2029 (1σ), 281 (1σ), and 319 (1σ) km in the downtrack, crosstrack, and out-of-plane directions, respectively, at E − 15. This orbit determination solution makes use of data through E − 16. If radiometric and onboard optical data between E − 16 and E − 15 and ground-based comet observations between E − 16 and E − 1 are included in the orbit determination solution, the probe position at Halley encounter can be determined to an accuracy of 1128 (1σ), 266 (1σ), and 271 (1σ) km in the downtrack, crosstrack, and out-of-plane directions, respectively. If radiometric and onboard optical data involving the main spacecraft, after the time of probe separation, are included in the probe orbit determination solution, a substantial further reduction in probe orbit determination errors relative to the comet can be achieved, due to the substantial improvement in the knowledge of the cometary ephemeris made possible with this data. Some rough estimates of the resulting probe orbit determination accuracies were presented in Ref. 12.

Table 4 Halley probe delivery parametric sensitivity study results

Deviation from baseline assumptions	Downtrack position uncertainty standard deviation at probe release mapped to encounter, km	Position standard deviation at encounter, km	
		Crosstrack	Out-of-plane
Baseline case	2029	322	365
1500-mm focal length spacecraft imaging system	2173	610	611
Onboard optical data frequency halved	2036	373	411
No onboard optical data	3814	1916	1383
Frequency of Earth-based observations of comet halved	2147	319	362
Earth-based comet observation data noise doubled	3193	319	360
No Earth-based comet observations	4774	316	358
A priori comet ephemeris uncertainty doubled	2275	306	357
No differenced multistation radiometric data	2033	359	442
Information lag doubled	2029	351	403
Navigation coast duration doubled	2021	307	305
Navigation coast eliminated	2137	416	606
Probe released 5 days earlier	2742	519	578
Thrust acceleration errors doubled—baseline values assumed in filter error model	2036	336	390
Nongravitational stochastic accelerations during coast arcs doubled—baseline values assumed in filter error model	2032	324	367
Probe separation velocity uncertainty doubled—baseline values assumed in filter error model	2029	323	366
Interval between control update computations doubled	2029	322	365
Interval over which control corrections are constant doubled	2029	322	365
Number of piecewise constant control corrections calculated at each control update doubled	2029	322	365
Feedback on estimated stochastic parameters included	2029	322	365

Navigation accuracy analysis results for ballistic missions to comet Halley have been presented in Refs. 10 and 16. The position errors at encounter stated here are significantly larger than those in Ref. 10, but are significantly smaller than those in Ref. 16. This is to be expected though, since the three missions are quite different in nature. Orbit determination data must terminate prior to probe separation at E − 15 days in the ion drive mission, if the rendezvous spacecraft is to be deflected away from the dust hazard zone. There is no corresponding requirement in the ballistic missions, so that orbit determination data much closer to encounter may be used in planning a final trajectory correction maneuver. However, the onboard imaging system assumed for the ion drive mission is better than that assumed for the ballistic mission in Ref. 10 and is much better than that assumed for the ballistic mission in Ref. 16. In addition, the ion drive mission and the ballistic mission in Ref. 16 assume preperihelion encounters with Comet Halley, while the ballistic mission in Ref. 10 assumes a postperihelion encounter, by which time the cometary ephemeris will be better known.

Parametric Sensitivity Studies for Halley Probe Delivery

In addition to the navigation accuracy analysis described above for the baseline navigation strategy, a study was carried out to determine the sensitivity of the navigation accuracy to changes in the navigation strategy and in various error modeling assumptions. The results of these parametric sensitivity studies will now be described. A total of 19 cases were considered, in addition to the baseline case. In each instance, all assumptions were exactly as in the baseline case, with one assumption changed. The 19 cases are described in Table 4. In this table, crosstrack and out-of-plane position standard deviations at encounter are presented, along with downtrack position uncertainty standard deviations at the time of the probe release, mapped to encounter.

One of the most important parameters investigated was the focal length of the onboard imaging system to be used for optical navigation. The 3000-mm focal length optics in the baseline design is a new system and is more massive and probably more expensive than the 1500-mm focal length optics used in several other interplanetary missions. Since the same charge-coupled device photodetector would be used regardless of the imaging system focal length, a halving of the focal length is, for the purposes of this study, equivalent to a doubling of the optical data noise and a doubling of the optical data biases. The crosstrack and out-of-plane position standard deviations at encounter are seen to nearly double, with this decrease in focal length. In addition, the cometary nucleus would be more difficult to detect at a range in excess of 75,000,000 km (the spacecraft/comet range at the time of probe separation) with the shorter focal length camera, a fact which is not taken into account in the accuracy analysis results. The accuracy analysis studies assume that optical navigation images of the postulated accuracy are always available when scheduled. For reference, each picture element of the 3000-mm focal length imaging system is 5×5 μrad in size. At a range of 75,000,000 km, this is equivalent to 375×375 km. For the 1500-mm focal length system, these numbers are doubled.

A halving of the frequency of onboard optical data (one frame per day between E − 50 and E − 40, two frames per day between E − 40 and E − 15) is seen to degrade probe delivery errors by about 15%. The complete elimination of onboard optical data causes these errors to increase by a factor of 4-6 and causes the downtrack position uncertainty to double as well. A halving of the frequency of the ground-based optical data (one observation every 10 days) has a negligible effect on the probe delivery accuracy. The time-of-encounter uncertainty is, however, affected slightly. A doubling of the noise in the ground-based optical data produces a 50% increase in the time-of-encounter uncertainty. The complete elimination of ground-based optical data has a negligible effect on probe delivery accuracy, but causes the downtrack

position uncertainty to more than double. A doubling of the a priori cometary ephemeris uncertainty degrades the time-of-encounter uncertainty, but, surprisingly, improves the probe delivery accuracy very slightly.

The complete elimination of multistation differenced radiometric data causes probe delivery errors to increase by 10-20%. Increasing the information lag associated with round-trip light time, orbit determination data processing, thrust vector command updating and sequence generation, etc., from 24 to 48 h causes about a 10% increase in probe delivery errors.

A doubling of the navigation coast length to 8 days (with the time of the trim maneuver unchanged) causes probe delivery errors to improve by 5-20%. The complete elimination of the navigation coast produces a much larger degradation in probe delivery accuracy. If the navigation coast length is held constant, but the probe is released 5 days earlier (20 days before encounter), probe delivery errors increase by about 65%.

If the thrust vector error standard deviations are, in actuality, twice as large as assumed in the orbit determination error model, both during the continuous thrusting phase and during the trim maneuver, the probe delivery errors increase by less than 10%. Very little degradation is observed if the level of stochastic nongravitational accelerations during coasting periods is doubled relative to the level assumed in the orbit determination error model. If the probe separation velocity errors are, in actuality, twice the level assumed in the orbit determination error model, the change in probe delivery accuracy is negligible.

The final parametric sensitivity study cases investigated involved changing certain aspects of the guidance strategy. One case involved the calculation of control history updates every 10 days instead of every 5 days. Another case involved the calculation of control corrections which are piecewise constant over 5-day, rather than 2½-days, intervals. In addition, the number of piecewise constant control corrections calculated at each control update time was doubled. (Some of these computed control corrections are never used, due to subsequent control update computations based upon improved orbit determination solutions.) Finally, feedback on estimated stochastic parameters was included in the guidance law. In all these cases, the probe delivery accuracy results were unchanged relative to the baseline.

Conclusion

Navigational feasibility of the Halley probe delivery portion of a Halley flyby/Tempel 2 rendezvous mission, making use of the solar electric propulsion system, has been demonstrated. For the baseline navigation system design, navigation strategy, and error modeling assumptions, the mean miss distance of the Halley probe relative to the cometary nucleus was found to be 394 km. The rms miss distance was found to be 487 km. The uncertainty in the time of encounter at the time of probe release was found to be 35.1 s (1σ). The sensitivities of the probe delivery accuracy and time-of-encounter uncertainty to parameters such as data frequencies, data accuracies (and imaging system focal length), stochastic acceleration modeling accuracies, trajectory time-line characteristics, information lag, and guidance algorithm parameters were investigated.

Acknowledgments

This paper presents the results of one phase of research carried out at the Jet Propulsion Laboratory, California Institute of Technology, under Contract NAS 7-100, sponsored by the National Aeronautics and Space Administration. The author would like to thank R. A. Jacobson for many helpful discussions regarding low-thrust navigation and S.L. Hast for his assistance in generating the numerical results presented here.

References

[1] Sauer Jr., C.G., "Trajectory Analysis and Performance for SEP Comet Encke Missions," AIAA Paper 73-1059, AIAA 10th Electric Propulsion Conference, Lake Tahoe, Nev., Oct.-Nov. 1973.

[2] McDanell, J.P., "Earth-Based Orbit Determination for Solar Electric Spacecraft with Application to a Comet Encke Rendezvous," AIAA Paper 73-174, AIAA 11th Aerospace Sciences Meeting, Washington, D.C., Jan. 1973.

[3] Jacobson, R.A., McDanell, J.P., and Rinker, G.C., "Use of Ballistic Arcs in Low Thrust Navigation," *Journal of Spacecraft and Rockets,* Vol. 12, March 1975, pp. 138-145.

[4] Boain, R.J., "A Mission Design for the Halley Comet Rendezvous Using Ion Drive," Paper 77-5, AAS/AIAA Astrodynamics Conference, Jackson, Wym., Sept. 1977.

[5] Thornton, C.L. and Jacobson, R.A., "Navigation Capability for an Ion Drive Rendezvous with Halley's Comet," *Journal of the Astronautical Sciences,* Vol. XXVI, July-Sept. 1978, pp. 197-210.

[6] Hastrup, R.C. and Sackett, L.L., "Design of a Dual Comet Ion Drive Mission," AIAA Paper 78-1435, AIAA/AAS Astrodynamics Conference, Palo Alto, Calif., Aug. 1978.

[7] Sackett, L.L., Hastrup, R.C., Yen, C.L., and Wood, L.J., "Comet Rendezvous Mission Design Using Solar Electric Propulsion," *Advances in the Astronautical Sciences,* Vol. 40, Pt. 1, 1979, pp. 343-372.

[8] *International Comet Mission: Halley/Tempel 2 Mission Baseline, Volume III. Comet Science Working Group Report,* NASA/ESA, JPL Internal Document 626-2, Vol. III, Nov. 1979.

[9] Boain, R.J. and Hastrup, R.C., "A Ballistic Mission to Fly By Comet Halley," AIAA Paper 80-1686, AIAA/AAS Astrodynamics Conference, Danvers, Mass., Aug. 1980.

[10] Wood, L.J., "Navigation Accuracy Analysis for a Halley Intercept Mission," AIAA Paper 81-0312, AIAA 19th Aerospace Sciences Meeting, St. Louis, Mo., Jan. 1981.

[11] Wood, L.J. and Krinik, A.C., "Navigation Accuracy Analyses for Two Comet Rendezvous Missions Using Ion Drive," AIAA Paper 80-1684, AIAA/AAS Astrodynamics Conference, Danvers, Mass., Aug. 1980.

[12] Wood, L.J. and Hast, S.L., "Navigation System Design for a Halley Flyby/Tempel 2 Rendezvous Mission Using Ion Drive," *Advances in the Astronautical Sciences,* Vol. 40, Pt. 1, 1979, pp. 49-78.

[13] Jacobson, R.A., "A Constrained Discrete Optimal Guidance Strategy for Low-Thrust Spacecraft," AAS/AIAA Astrodynamics Conference, Vail, Colo., July 1973.

[14] Jacobson, R.A., "Limited Variance Control in Statistical Low Thrust Guidance Analysis," Paper 75-066, AAS/AIAA Astrodynamics Conference, Nassau, Bahamas, July 1975.

[15] Rinker, G.C., Jacobson, R.A., and Wood, L.J., "Statistical Analysis of Trim Maneuvers in Low-Thrust Interplanetary Navigation," *Journal of Spacecraft and Rockets,* Vol. 13, Aug. 1976, pp. 509-512.

[16] Farquhar, R.W., Muhonen, D.P., Mann, F.I., Wooden, W.H., and Yeomans, D.K., "Shuttle-Launched Multi-Comet Mission 1985," Paper 75-085, AAS/AIAA Astrodynamics Conference, Nassau, Bahamas, July 1975.